Atmospheric Research 161–162 (2015) 134–142

Contents lists available at ScienceDirect

Atmospheric Research

journal homepage: www.elsevier.com/locate/atmos

Size-resolved airborne particulate oxalic and related secondary organic aerosol species in the urban atmosphere of Chengdu, China

Chunlei Cheng [a,b,c], Gehui Wang [a,b,d,*], Jingjing Meng [a,b], Qiyuan Wang [a,b], Junji Cao [a,b], Jianjun Li [a,b], Jiayuan Wang [a,b,c]

[a] Key Lab of Aerosol Chemistry & Physics, Institute of Earth Environment, Chinese Academy of Sciences, Xi'an 710061, China
[b] State Key Laboratory of Loess and Quaternary Geology, Institute of Earth Environment, Chinese Academy of Sciences, Xi'an 710061, China
[c] University of Chinese Academy of Sciences, Beijing 100049, China
[d] Department of Environmental Science, Xi'an Jiaotong University, Xi'an 710049, China

ARTICLE INFO

Article history:
Received 29 September 2014
Received in revised form 31 March 2015
Accepted 10 April 2015
Available online 16 April 2015

Keywords:
Size distribution
Secondary organic aerosols
Aqueous phase chemistry
Liquid water content
Biomass burning

ABSTRACT

Size-segregated (9-stages) airborne particles during winter in Chengdu city of China were collected on a day/night basis and determined for dicarboxylic acids (diacids), ketocarboxylic acids (ketoacids), α-dicarbonyls, inorganic ions, and water-soluble organic carbon and nitrogen (WSOC and WSON). Diacid concentration was higher in nighttime (1831 ± 607 ng m^{-3}) than in daytime (1532 ± 196 ng m^{-3}), whereas ketoacids and dicarbonyls showed little diurnal difference. Most of the organic compounds were enriched in the fine mode (<2.1 μm) with a peak at the size range of 0.7–2.1 μm. In contrast, phthalic acid (Ph) and glyoxal (Gly) presented two equivalent peaks in the fine and coarse modes, which is at least in part due to the gas-phase oxidation of precursors and a subsequent partitioning into pre-existing particles. Liquid water content (LWC) of the fine mode particles was three times higher in nighttime than in daytime. The calculated in-situ pH (pH_{is}) indicated that all the fine mode aerosols were acidic during the sampling period and more acidic in daytime than in nighttime. Robust correlations of the ratios of glyoxal/oxalic acid (Gly/C_2) and glyoxylic acid/oxalic acid ($\omega C_2/C_2$) with LWC in the samples suggest that the enhancement of LWC is favorable for oxidation of Gly and ωC_2 to produce C_2. Abundant K^+ and Cl^- in the fine mode particles and the strong correlations of K^+ with WSOC, WSON and C_2 indicate that secondary organic aerosols in the city are significantly affected by biomass burning emission.
© 2015 Elsevier B.V. All rights reserved.

1. Introduction

Organic aerosol (OA) is a large fraction of atmospheric fine particles (Jimenez et al., 2009) and involves many atmospheric processes, such as nucleation and particle growth, solar radiation reflection, cloud condensation nuclei (CCN) formation and visibility reduction (Lim and Turpin, 2002). The dominant part of OA (up to 90% in urban areas) (Kalberer et al., 2004) is secondary organic aerosols (SOAs), which are formed through homogenous oxidation of gas-phase species followed by subsequent partitioning into pre-existing particles or heterogeneous reaction of gas precursors with particles (Shiraiwa et al., 2013). Dicarboxylic acids and their precursors, e.g., ketocarboxylic acids and α-dicarbonyls, are important classes of SOA, because they are abundant and ubiquitous in the atmosphere. In the urban atmosphere primary emissions of dicarboxylic acids, ketocarboxylic acid and α-dicarbonyls from vehicle exhausts and industrial activities are minor (Huang and Yu, 2007; Stone et al., 2010), while they are largely derived from secondary oxidation.

Haze events have frequently occurred in many Chinese cities since the 1990s due to rapid economy expansion and urbanization (Zhang et al., 2012). Sichuan Basin, which is located in the southwestern part of China (Supplementary Fig. S1), is one of the most polluted regions in the world. Satellite observation showed that annual mean $PM_{2.5}$ in 2001–2006 in Sichuan Basin was more than 80 μg m^{-3} (van Donkelaar et al., 2010), which is seven times higher than the WHO annual average (10 μg m^{-3}). The basin-like topography is favorable for aerosol formation and accumulation in the region, especially in winter when pollutant emissions are enhanced due to house heating. A few studies have found that biomass burning is an important source of airborne particles in Sichuan Basin, in addition to traffic exhausts, industrial activity and road dust (Tao et al., 2013; Wang et al., 2006). A recent modeling work demonstrated that Sichuan Basin is one of the regions with the highest sulfate concentration in China (Wang et al., 2013c). Chengdu is a major city in Sichuan Basin and located in its western part, (Supplementary Fig. S1). High level of particles has been a persistent problem in the city (Wang et al., 2013b). In the current work we focus on the wintertime SOA in Chengdu city in order to improve our

* Corresponding author at: State Key Laboratory of Loess and Quaternary Geology, Institute of Earth Environment, Chinese Academy of Sciences, Xi'an 710061, China. Tel.: +86 29 6233 6277; fax: +86 29 6233 6234.
E-mail address: wanggh@ieecas.cn (G. Wang).

http://dx.doi.org/10.1016/j.atmosres.2015.04.010
0169-8095/© 2015 Elsevier B.V. All rights reserved.

understanding on the origins of haze formation in China. First, we investigate the diurnal variations in compositions and concentrations of SOA (i.e., dicarboxylic acids, ketocarboxylic acids and α-dicarbonyls), inorganic ions and water-soluble organic carbon and nitrogen in the size-resolved samples collected in Chengdu city. Then we analyze their size distributions and the role of the aerosol liquid water content to discuss their formation mechanisms. Finally we explore the influence of biomass burning on the SOA productions.

2. Sampling and analysis

2.1. Sample collection

Eight sets of size-segregated samples were collected by using a nine-stage Andersen impactor sampler (Series 20-800, Thermo Electron Corporation USA) at a flow rate of 28.3 L min^{-1} from January 5th to 24th, 2011 on the rooftop of Institute of Plateau Meteorology (about 20 m above the ground), which is located at the downtown area of Chengdu. All samples were collected onto a pre-combusted quartz fiber filter (450 °C for 8 h, Φ80 mm). Four sets of the size-segregated samples were collected in daytime from 7:00 to 18:30 and another four sets were collected at night from 19:00 to 6:30 (Table 1). Airflow rate of the sampler was regulated with the flow meter made by the sampler manufacturer before and after sampling. The cutoff points of the size-resolving sampler are 0.4, 0.7, 1.1, 2.1, 3.3, 4.7, 5.8 and 9.0 μm, respectively (Wang et al., 2012b). Two sets of field blank samples were collected separately before and after the sampling for about 20 min by mounting blank filters onto the sampler without sucking any air. All the samples were determined for particle mass concentration by weighing the filter mass before and after sampling using a Sartorius MC5 electronic microbalance with ± 1 μg sensitivity (Sartorius, Göttingen, Germany) after a 48 h equilibration in a glass chamber (T: 25 ± 0.5 °C, RH: 35 ± 2%). All the sample filters were sealed individually in an aluminum foil bag and stored at −20 °C prior to analysis. Meteorological data during the sampling periods were collected and are presented in Supplementary Fig. S2.

2.2. Sample analysis

2.2.1. Water-soluble organic carbon (WSOC), water-soluble organic nitrogen (WSON) and inorganic ions

Detailed analytical procedures of WSOC, WSON and inorganic ions have been reported in previous work (Meng et al., 2013; Wang et al., 2013a). Briefly, one fourth of the filter was cut into pieces, extracted with Milli-Q water for three times and filtered using a PTFE filter to remove particles and filter debris. Then the combined water-extracts were analyzed for WSOC and WSON by using a Shimadzu TOC/TON-5000 Analyzer and inorganic ions by using a Dionex 600 ion chromatography system (Sunnyvale, CA).

2.2.2. Dicarboxylic acids and related organic compounds

An analytical method for dicarboxylic acids, ketocarboxylic acids and α-dicarbonyls was reported previously (Wang et al., 2012a). Briefly, one fourth of the filter was ultrasonically extracted with Milli-Q water for three times, then concentrated to dryness by rotary evaporation under vacuum condition at 60 °C and reacted with 14% BF_3/butanol mixture at 100 °C for 1 h. Afterward, the derivatized sample was added with *n*-hexane and extracted with pure water for three times. Finally the hexane layer was concentrated to 100 μL by nitrogen blow and quantified by gas chromatography (GC) coupled with a FID detector. The GC oven temperature was programmed from 50 °C to 120 °C at a rate of 30 °C min^{-1}, and then to 300 °C at a rate of 6 °C min^{-1} with a final hold at 300 °C for 10 min. All detected compounds were confirmed by GC–MS (Agilent, GC7890A–MS5975C). Recoveries of the target compounds were 80–85% for oxalic acid and 92–115% for others. Target compounds in the field blanks were less than 5% of the ones in the real samples. Data reported here were corrected by field blank samples but not corrected by the recoveries.

2.2.3. Liquid water content (LWC) and in-situ pH (pH_{is})

LWC was calculated using the Extended AIM Aerosol Thermodynamics Model (Wexler and Clegg, 2002). Because the mode does not include Ca^{2+} and Mg^{2+}, which are abundant in the coarse mode (>2.1 μm) of samples, here we only calculated LWC for the fine mode (<2.1 μm) samples. Concentrations of Na^+, Cl^-, Br^- and organic acids are much lower in the fine mode samples compared to SO_4^{2-}, NO_3^- and NH_4^+. Thus, the Model II is suitable for the LWC calculation (Clegg et al., 1998). Particle in-situ acidity (pH_{is}) was also calculated through the Model II with the following equation (Xue et al., 2011):

$$pH_{is} = -\log\alpha_{H^+} = -\log\left(\gamma_{H^+} \times n_{H^+} \times \frac{1000}{V_a}\right)$$

where n_{H^+} and γ_{H^+} are determined by the Model II, n_{H^+} is the concentration of free H^+ (mol m^{-3}) in aqueous phase of particles and γ_{H^+} is the activity coefficient of H^+, while V_a is the volume concentration of the H_2O (cm^3 m^{-3}).

3. Results and discussion

3.1. Molecular compositions of dicarboxylic acids, ketocarboxylic acids and α-dicarbonyls in the daytime and nighttime samples

A homologous series of dicarboxylic acids (C_2–C_{11}), ketocarboxylic acids and α-dicarbonyls in the Chengdu samples were determined (Table 2). TSP (total suspended particles)-equivalent concentrations (the sum of concentrations on the nine stages) of dicarboxylic acids ranged from 1258 to 1716 ng m^{-3} with an average of 1532 ng m^{-3} in daytime and from 1255 to 2676 ng m^{-3} with an average of 1831 ng m^{-3} in nighttime. Diacids in Chengdu are comparable to those in Xi'an, China (1843 ± 810 ng m^{-3}) (Cheng et al., 2013) but much

Table 1
Meteorological parameters (Ave. ± Std) during the 2011 wintertime campaign in Chengdu.

Sample set	Day[a] (dd/mm–dd/mm)	RH (%)[b]	T (°C)[b]	WS (m s^{-1})[b]	Sample set	Night[a] (dd/mm–dd/mm)	RH (%)[b]	T (°C)[b]	WS (m s^{-1})[b]
1st	05/01–09/01	54 ± 18 (28–85)	5.6 ± 1.6 (2.5–8.2)	0.7 ± 0.2 (0.3–1.2)	2nd	05/01–09/01	67 ± 12 (36–86)	4.4 ± 0.9 (2.5–6.5)	0.6 ± 0.3 (0.1–1.4)
3rd	10/01–14/01	58 ± 14 (28–80)	5.1 ± 2.1 (1.2–8.6)	0.8 ± 0.3 (0.3–1.3)	4th	10/01–14/01	68 ± 9 (41–82)	4.0 ± 1.5 (1.2–6.9)	0.6 ± 0.3 (0.2–1.4)
5th	15/01–19/01	65 ± 20 (22–86)	3.6 ± 2.0 (0.7–9.0)	0.8 ± 0.2 (0.2–1.2)	6th	15/01–19/01	75 ± 13 (32–86)	2.6 ± 1.5 (0.5–6.7)	0.6 ± 0.3 (0.2–1.6)
7th	20/01–24/01	65 ± 12 (44–84)	4.8 ± 1.8 (0.7–8.6)	0.6 ± 0.2 (0.2–1.2)	8th	20/01–24/01	71 ± 9 (51–85)	3.7 ± 1.0 (1.7–6.2)	0.5 ± 0.2 (0.2–0.9)

[a] Day: 07:00–18:30, night: 19:00–06:30.
[b] RH: relative humidity, T: temperature, and WS: wind speed.

Table 2
Total suspended particle (TSP)-equivalent concentrations (the sum of concentrations on the nine stages) of dicarboxylic acids, ketocarboxylic acids, α-dicarbonyls, inorganic ions, water soluble organic carbon (WSOC) and nitrogen (WSON), liquid water content (LWC) and in-situ pH (pH_{is}) in Chengdu in winter.

Compounds	Day (N = 4)	Night (N = 4)
	Ave. ± Std. (Min–Max)	Ave. ± Std. (Min–Max)
I. Dicarboxylic acids, ng m^{-3}		
Oxalic, C_2	686 ± 114 (536–809)	862 ± 345 (557–1343)
Malonic, C_3	136 ± 39 (79–167)	147 ± 66 (83–218)
Succinic, C_4	145 ± 33 (109–184)	187 ± 55 (120–239)
Glutaric, C_5	26 ± 9.1 (15–36)	37 ± 15 (22–52)
Adipic, C_6	14 ± 5.0 (9.4–20)	13 ± 6.9 (5.2–22)
Pimelic, C_7	14 ± 6.8 (8.4–24)	12 ± 2.3 (9.2–15)
Suberic, C_8	7.9 ± 1.9 (5.5–10)	7.6 ± 3.7 (3.5–11)
Azelaic, C_9	26 ± 11 (16–42)	37 ± 15 (23–52)
Sebacic, C_{10}	2.7 ± 0.7 (1.8–3.5)	3.7 ± 1.3 (2.4–5.4)
Undecanedioic, C_{11}	1.1 ± 0.5 (0.7–1.8)	1.7 ± 1.2 (0.9–3.4)
Methylmalonic, iC_4	14 ± 1.3 (13–16)	18 ± 6.6 (12–27)
Methylsuccinic, iC_5	19 ± 2.9 (15–21)	25 ± 7.9 (15–32)
Methylglutaric, iC_6	2.3 ± 0.5 (1.6–2.7)	2.5 ± 0.8 (1.8–3.2)
Maleic, M	28 ± 3.6 (23–32)	28 ± 8.2 (21–40)
Fumaric, F	14 ± 7.0 (4.1–20)	17 ± 11 (8.5–32)
Methylmaleic, mM	11 ± 4.2 (8.4–18)	11 ± 3.7 (7.6–16)
Phthalic, Ph	274 ± 39 (243–325)	264 ± 72 (200–367)
Isophthalic, iPh	7.7 ± 1.7 (5.9–9.4)	6.8 ± 1.6 (5.8–9.2)
Terephthalic, tPh	94 ± 35 (64–144)	137 ± 57 (82–202)
Ketomalonic, κC_3	6.4 ± 11 (0.4–23)	8.5 ± 8.9 (2.2–21)
4-Ketopimelic, κC_7	4.3 ± 1.5 (3.1–6.1)	4.0 ± 2.4 (2.3–7.6)
Subtotal	1532 ± 196 (1258–1716)	1831 ± 607 (1255–2676)
II. Ketocarboxylic acids, ng m^{-3}		
Pyruvic, Pyr	115 ± 17 (99–138)	99 ± 16 (81–115)
Glyoxylic, ωC_2	90 ± 16 (67–103)	91 ± 23 (69–124)
3-Oxopropanoic, ωC_3	12 ± 1.2 (11–14)	10 ± 3.5 (6.8–15)
4-Oxabutanoic, ωC_4	25 ± 2.7 (22–27)	20 ± 7.5 (12–30)
9-Oxononanoic, ωC_9	9.2 ± 2.8 (5.7–12.2)	9.4 ± 1.2 (7.6–10.6)
Subtotal	250 ± 27 (224–287)	229 ± 42 (196–286)
III. α-Dicarbonyls, ng m^{-3}		
Glyoxal, Gly	61 ± 4.2 (55–64)	53 ± 10 (41–61)
Methylglyoxal, mGly	53 ± 5.5 (48–60)	54 ± 14 (38–66)
Subtotal	113 ± 7.9 (107–125)	107 ± 17 (86–127)
IV. Inorganic ions, μg m^{-3}		
F^-	0.4 ± 0.3 (0.2–0.8)	0.4 ± 0.3 (0.2–0.8)
Cl^-	2.7 ± 0.9 (1.5–3.5)	4.7 ± 1.9 (3.1–7.1)
NO_3^-	15 ± 2.8 (11–17)	18 ± 3.1 (14–21)
SO_4^{2-}	27 ± 6.0 (18–32)	31 ± 5.3 (26–36)
Na^+	2.1 ± 1.3 (1.1–4.1)	2.3 ± 1.4 (1.4–4.3)
NH_4^+	9.5 ± 2.2 (6.3–11)	12 ± 2.9 (8.8–15)
K^+	1.3 ± 0.4 (0.7–1.6)	2.0 ± 0.7 (1.2–2.7)
Mg^{2+}	0.3 ± 0.1 (0.2–0.3)	0.3 ± 0.1 (0.2–0.4)
Ca^{2+}	3.7 ± 1.1 (2.5–4.8)	3.6 ± 1.3 (2.2–5.4)
Subtotal	62 ± 14 (42–74)	74 ± 16 (58–90)
V. Others, μg m^{-3}		
WSOC	20 ± 4.3 (15–25)	23 ± 4.4 (17–27)
WSON	5.6 ± 1.1 (3.9–6.5)	7.2 ± 1.8 (5.5–9.7)
LWC[a]	13 ± 5.8 (7.5–18)	35 ± 7 (27–42)
pH_{is}[a]	−1.2 ± 1.1 (−2.3–0.3)	0.7 ± 1.0 (−0.2–2.1)
TSP mass	423 ± 31 (377–444)	471 ± 42 (408–495)

[a] Calculated only for the fine mode of samples (<2.1 μm).

higher than those in other Chinese cities (Ho et al., 2007), indicating severe air pollution problem in Chengdu. Being similar to that in other cities of China (Ho et al., 2007), oxalic acid (C_2) is the dominant species in Chengdu and accounts for 45 ± 7.4% of the total diacids in daytime and 47 ± 19% of the total at night, respectively (Fig. 1). TSP-equivalent concentrations of ketocarboxylic acids were 250 ± 27 and 229 ± 42 ng m^{-3} in the daytime and nighttime samples, respectively, among which pyruvic acid (Pyr) and glyoxylic (ωC_2) are the dominant species, accounting for about 80% of the total ketoacids (Table 2). Glyoxal (Gly) and methylglyoxal (mGly) showed similar levels in Chengdu and no significant diurnal difference was found for both dicarbonyls (Table 2). As shown in Fig. 1, oxalic (C_2), malonic (C_3), succinic (C_4), glutaric (C_5), azelaic (C_9) and terephthalic (tPh) acids exhibited higher concentrations in nighttime, while phthalic acid (Ph) and Pyr presented higher concentrations in daytime.

Molecular compositions of diacids are influenced by photochemical process and source strength (anthropogenic vs. biogenic sources) (Kawamura et al., 2012, 2013). Ratio of C_3/C_4 (Table 3) is useful for evaluation of photochemical oxidation degree since C_3 is produced from C_4 by photochemical oxidation (Kawamura and Ikushima, 1993). Compared with that in nighttime (0.81 ± 0.32), the higher ratio of C_3/C_4 in daytime (1.00 ± 0.29) implied a strong photochemical oxidation (Yang et al., 2008). Both ratios of C_6/C_9 and Ph/C_9 are indicative of the relative strength of anthropogenic sources to biogenic sources (Cheng et al., 2013), because C_6 and Ph in urban regions are mostly produced from oxidation of cyclohexene and aromatic hydrocarbons, which originate from human activities. In contrast, C_9 is formed through oxidation of biogenic unsaturated fatty acids (e.g., oleic acid) (Wang et al., 2010, 2011). In comparison with those (0.33 ± 0.10 and 7.9 ± 2.9, Table 3) in nighttime, the higher ratios of C_6/C_9 and Ph/C_9 (0.60 ± 0.20 and 12 ± 4.6, Table 3) in daytime are attributed to intensive anthropogenic emissions.

3.2. Size distributions of dicarboxylic acids, ketocarboxylic acids and α-dicarbonyls in daytime and nighttime samples

To further discuss the formation process of secondary organic aerosols, diurnal differences in size distributions of major diacids, ketoacids and α-dicarbonyls in the samples are displayed in Fig. 2. C_2 and C_4 presented a monomodal pattern both in day and night with a dominant peak in the fine mode (<2.1 μm) (Fig. 2a and c), which are similar to those in other Asian cities (Agarwal et al., 2010; Wang et al., 2012a). C_3 exhibited a bimodal pattern during the whole sampling period with a large peak in the fine mode and a minor peak in the coarse mode (>2.1 μm) (Fig. 2b). The relatively more abundant C_3 in the coarse mode is most likely due to higher vapor pressure of C_3 compared to C_4 (C_3: 1.0×10^{-5} Torr; C_4: 6.9×10^{-7} Torr) (Prenni et al., 2001). Ph displayed two equivalent peaks in the fine and coarse modes (Fig. 2d). The coarse mode of Ph accounts for 52 ± 2% of the total mass in the whole size range in daytime and 37 ± 15% of the total in nighttime, respectively. In urban area airborne particulate Ph is produced from photochemical oxidation of naphthalene in the gas phase and subsequent adsorption onto pre-existing particles (Wang et al., 2012a). In comparison with that in nighttime the relatively more abundant coarse mode of Ph in daytime is most likely caused by more dust. As seen in Fig. 2g and h, both Gly and mGly displayed a bimodal pattern, but Gly presented two equivalent peaks in the fine and coarse modes while mGly was dominant in the fine mode. Gly and mGly are produced from the gas phase oxidation of volatile organic compounds (VOCs), and followed by a subsequent partitioning into the particle phase (Myriokefalitakis et al., 2011). The particle phase Gly and mGly undergo a further oxidation to produce Pyr and ωC_2; the latter compounds exhibited identical bimodal size distribution pattern in Chengdu during the campaign (Fig. 2e and f). Geometric mean diameters (GMDs) of the major organic compounds and inorganic ions are presented in Table 4. Being similar to those of SO_4^{2-}, NO_3^- and NH_4^+, GMDs of the fine mode of C_2 and C_3 are around 10% larger in nighttime, which can be explained by an enhanced hygroscopic growth of particles at night due to the higher RH (Table 1).

3.3. Influence of liquid water content (LWC) on the abundance and composition of diacids and other water-soluble species

The descending of boundary layer (BL) height at night can result in an accumulation of aerosols within the BL, possibly leading to the enrichment of diacids and other species. However, the higher relative abundance of diacids in particle mass and WSOC in nighttime cannot

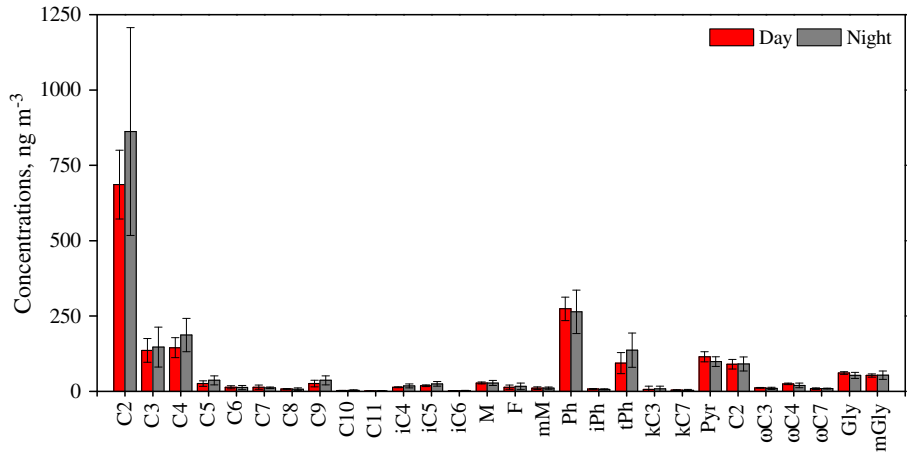

Fig. 1. Diurnal variations in ambient concentrations of dicarboxylic acids, ketocarboxylic acids and α-dicarbonyls in Chengdu in winter.

be explained by the BL height change (Miyazaki et al., 2009). Relative abundance of C_2 in total diacids is an indicator of aerosol aging degree (Pavuluri et al., 2010). With respect to the Chengdu samples no significant diurnal difference in relative abundance of C_2/total diacids was observed, which suggests that the nighttime aerosols were also aged (Table 3). The abundant diacids during the nighttime were probably associated with an enhanced aqueous phase oxidation (van Pinxteren et al., 2014) or more precursors emitted from biomass burning. The aqueous phase formation of diacids has been reported in previous studies (Ervens et al., 2014; Lim et al., 2005), but detailed formation mechanism remains unclear. Here we investigate the impact of liquid water content (LWC) of particles on the formation of diacids in the city.

Based on the Extended AIM Aerosol Thermodynamics Model (Wexler and Clegg, 2002), LWC and particle in-situ acidity (pH_{is}) of the fine mode samples (<2.1 μm) were calculated (Fig. 3). Higher abundance of LWC at night was mainly ascribed to the enhancement of relative humidity (RH) (Table 1), since there was no significant change in relative abundance of SO_4^{2-}, NO_3^- and NH_4^+ in the fine mode aerosols (Supplementary Table S1), which are the major hygroscopic species in the atmosphere. LWC of the fine mode particles was three times higher in nighttime than in daytime, and the highest LWC was found in the size of 0.7–1.1 μm in daytime and in the larger size of 1.1–2.1 μm in nighttime. The calculated pH_{is} indicated that all the fine mode aerosols were acidic during the whole sampling period and more acidic in daytime than in nighttime (Fig. 3). Diurnal changes of pH_{is} in the fine particles mainly depend on RH, because little difference was found for the diurnal abundance of SO_4^{2-}, NO_3^- and NH_4^+.

Fig. 4 shows the abundances of C_2, diacids, ketoacids and α-dicarbonyls relative to WSOC in the fine mode (<2.1 μm). For the nighttime samples the abundances of C_2 and total diacids relative to WSOC increased along with an increase in LWC (Fig. 4a and b), indicating that the aqueous phase oxidation may be enhanced under higher RH condition since LWC often positively correlates with RH. However, the abundances of ketocarboxylic acids and α-dicarbonyls relative to WSOC in nighttime are lower compared to those in daytime (Fig. 4c and d). Due to high Henry's Law constants (K_H), α-dicarbonyls (Gly and mGly) are easily hydrated and partitioned into the aerosol phase with lifetime less than 3 h (Kampf et al., 2012; Vrekoussis et al., 2009; Yasmeen et al., 2010), radical oxidation of α-dicarbonyls in aqueous phase leads to formation of ketoacids (C_2 and Pyr) that are further oxidized to oxalic acid (C_2) (Lim et al., 2010; Tan et al., 2010; Wang et al., 2012a). Production of ketoacids and α-dicarbonyls from photo-oxidation of VOCs is inhibited in nighttime due to no solar radiation, on the other hand, the increased LWC in nighttime is favorable for aqueous phase oxidation of ketoacids and α-dicarbonyls to produce oxalic acid (Jia and Xu, 2014). Thus, relative abundances of ketocarboxylic acids and α-dicarbonyls to WSOC in the fine mode samples were lower at night (Fig. 4c and d). The larger decreases in relative abundances of ketoacids to WSOC than those of α-dicarbonyls in nighttime were observed, which is probably due to the less acidity of the aqueous phase ($pH_{is} = 0.7 \pm 1.0$ in nighttime versus -1.2 ± 1.1 in daytime) (Table 2). It has been proposed that the aqueous oxidation of ωC_2 to C_2 is more efficient at higher pH conditions, because the reaction rate of glyoxylate anion (ωC_2^-) is one order of magnitude higher than that of ωC_2 (Ervens et al., 2003, 2011).

The ratios of Gly/C_2 and $\omega C_2/C_2$ are used here to investigate the oxidation degree from Gly and ωC_2 to C_2. Fig. 5a and b shows the correlations of Gly/C_2 and $\omega C_2/C_2$ with LWC in the fine mode samples. The more significant correlations of the nighttime samples suggest that the enhancement of LWC at night is favorable for C_2 production from Gly and ωC_2. A strong positive correlation was found for the C_2/diacids and LWC ($r^2 = 0.68$, $p < 0.01$) in nighttime (Fig. 5c), again confirming that an increase in LWC favors C_2 production. Moreover, relative abundance of sulfate in particle mass (SO_4^{2-}/PM) also showed a robust positive correlation with LWC at night ($r^2 = 0.88$, $p < 0.01$) (Fig. 5d), indicating that an increase in LWC is favorable for aqueous phase production of sulfate. However, no correlation between C_2 and LWC was found for the nighttime samples, because C_2 is produced by various aqueous reactions (e.g., oxidation and decomposition) that are effected by many factors such as LWC, acidity and ion strength (Cheng et al., 2013).

NH_4^+, NO_3^- and WSON showed higher concentrations in nighttime (Table 2), and all exhibited a monomodal pattern with a peak in the fine mode (Supplementary Fig. S3). NH_4^+, NO_3^- and WSON showed stronger correlations with LWC in nighttime than in daytime (Fig. 6a, b, and c). The most abundant species of WSON in the atmosphere are the low molecular weight aliphatic amines such as methylamine, dimethylamine, ethylamine, and diethylamine (Ge et al., 2011a). Although these amines have high vapor pressure, they are highly water-soluble. The dissolution and acid–base reaction of aliphatic amine with sulfuric and nitric acids are the major formation pathways

Table 3
Diurnal mass ratios (Ave. ± Std) of diacids in total suspended particle (TSP)-equivalent concentrations (the sum of concentrations on the nine stages) in Chengdu[a].

	C_2/diacids	C_3/C_4	C_6/C_9	Ph/C_9
Day	0.45 ± 0.02	1.0 ± 0.29	0.60 ± 0.20	12 ± 4.6
Night	0.46 ± 0.03	0.81 ± 0.32	0.33 ± 0.10	7.9 ± 2.9

[a] For compound abbreviations, see Table 2.

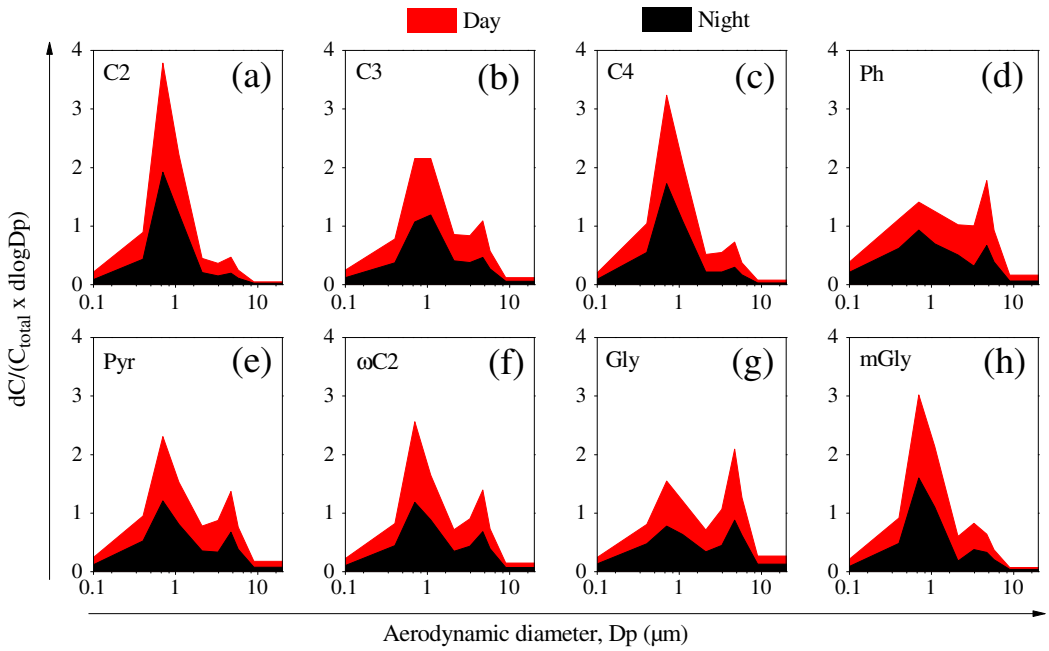

Fig. 2. Diurnal size distributions of dicarboxylic acids and related compounds in Chengdu: (a) oxalic acid (C_2), (b) malonic acid (C_3), (c) succinic acid (C_4), (d) phthalic acid (Ph), (e) pyruvic acid (Pyr), (f) glyoxylic acid (ωC_2), (g) glyoxal (Gly), and (h) methylglyoxal (mGly).

of airborne particulate WSON (Sellegri et al., 2005). Henry's law coefficients of amines increase sharply with the decrease of aerosol pH (Ge et al., 2011b), and thus acidic aerosols are favorable for the gas-to-particle phase partitioning of NH_3 and amines. Because amines are of stronger basicity than ammonium, amines can replace ammonium from ammonium sulfate and ammonium nitrate salts (Lloyd et al., 2009; Malloy et al., 2009; Silva et al., 2008). Salo et al. (Salo et al., 2011) investigated the thermal characteristics of aminium nitrate nanoparticles and found that the enthalpy of vaporization for aminium nitrates ranges from 54 kJ mol^{-1} to 74 kJ mol^{-1} with the vapor pressures at 298 K around 10^{-4} Pa. These values suggest that aminium nitrates can partition into the aerosol phase. The enhancement of LWC is favorable for the dissolution and partitioning of amines into the aqueous phase, leading to an increase of WSON with an increase in LWC. It was reported that reactive uptake of Gly on ammonium sulfate seed aerosols led to production of imidazole under dark and irradiated conditions (Galloway et al., 2009). For the Chengdu nighttime samples, the lower mass fraction of Gly is probably associated with the formation of imidazole, which also contributes to WSON.

3.4. Impact of biomass burning emission on secondary organic aerosols (SOAs)

Biomass burning has been found as an important source of atmospheric inorganic pollutants in Chengdu city (Tao et al., 2013; Yang et al., 2012). K^+ is considered as an important tracer for biomass burning plumes (Falkovich et al., 2005). Both soil dust and biomass burning are the sources of K^+, but K^+ in fine particles is mostly derived from biomass burning (Andreae, 1983). Diurnal size distributions showed that K^+ in the Chengdu samples was enriched in the fine mode (<2.1 μm) with a peak at the size range of 1.1–2.1 μm (Supplementary Fig. S3), indicating that the fine mode of K^+ in the city is largely derived from biomass burning. The fine mode of K^+ was 1.2 ± 0.4 μg m^{-3} in daytime and 1.9 ± 0.6 μg m^{-3} in nighttime, while the relative abundance of K^+ to particle mass in the fine mode (<2.1 μm) was 0.54 ± 0.13% and 0.74 ± 0.20% during the day and night, respectively. In comparison with those in daytime the higher concentrations and relative abundances of K^+ clearly indicate stronger biomass burning emission at night in the city, which is in agreement with a previous study (Li et al.,

Table 4
Geometric mean diameters (GMD, μm) (Ave. ± Std) of main components in the fine (<2.1 μm) and coarse (>2.1 μm) modes and the total size range in Chengdu[a].

	Day			Night			Day/night		
	Fine	Coarse	Total	Fine	Coarse	Total	Fine	Coarse	Total
C_2	0.90 ± 0.08	6.6 ± 1.1	1.2 ± 0.04	0.99 ± 0.01	6.8 ± 1.2	1.3 ± 0.1	0.92	0.97	0.96
C_3	0.91 ± 0.03	6.9 ± 1.1	1.8 ± 0.2	1.01 ± 0.10	7.1 ± 0.8	1.9 ± 0.7	0.90	0.97	0.91
C_4	0.93 ± 0.06	7.4 ± 1.1	1.6 ± 0.2	0.95 ± 0.03	7.1 ± 0.9	1.4 ± 0.2	0.98	1.04	1.14
C_9	0.83 ± 0.05	4.7 ± 0.9	1.1 ± 0.04	0.82 ± 0.01	3.9 ± 1.1	1.0 ± 0.1	1.00	1.18	1.06
Ph	0.72 ± 0.03	7.6 ± 0.3	2.4 ± 0.1	0.76 ± 0.06	6.9 ± 1.9	1.8 ± 0.7	0.94	1.09	1.33
Pyr	0.86 ± 0.07	8.3 ± 1.5	2.2 ± 0.4	0.87 ± 0.01	8.3 ± 0.2	1.9 ± 0.3	0.99	1.01	1.15
ωC_2	0.88 ± 0.05	7.7 ± 0.6	1.9 ± 0.2	0.91 ± 0.01	7.8 ± 0.8	2.0 ± 0.4	0.97	0.99	0.94
Gly	0.84 ± 0.06	9.1 ± 0.6	3.1 ± 0.1	0.81 ± 0.03	9.7 ± 1.2	2.8 ± 0.9	1.03	0.93	1.10
mGly	0.93 ± 0.06	5.9 ± 0.9	1.5 ± 0.2	0.96 ± 0.05	7.6 ± 1.2	1.5 ± 0.1	0.96	0.77	1.00
Cl^-	0.83 ± 0.09	8.9 ± 1.1	1.2 ± 0.2	0.90 ± 0.07	7.5 ± 0.9	1.2 ± 0.1	0.92	1.18	0.99
NO_3^-	0.84 ± 0.07	6.6 ± 0.9	1.3 ± 0.2	0.94 ± 0.05	6.5 ± 0.7	1.4 ± 0.1	0.89	1.02	0.93
SO_4^{2-}	0.93 ± 0.08	7.0 ± 0.5	1.4 ± 0.2	1.02 ± 0.06	6.7 ± 0.6	1.5 ± 0.02	0.91	1.04	0.99
NH_4^+	0.88 ± 0.08	4.4 ± 0.6	1.0 ± 0.1	0.97 ± 0.06	4.3 ± 0.7	1.1 ± 0.04	0.91	1.04	0.92
K^+	0.89 ± 0.11	3.6 ± 0.8	1.0 ± 0.1	0.91 ± 0.05	4.3 ± 1.4	1.0 ± 0.1	0.97	0.84	0.96

[a] For compound abbreviations, see Table 2.

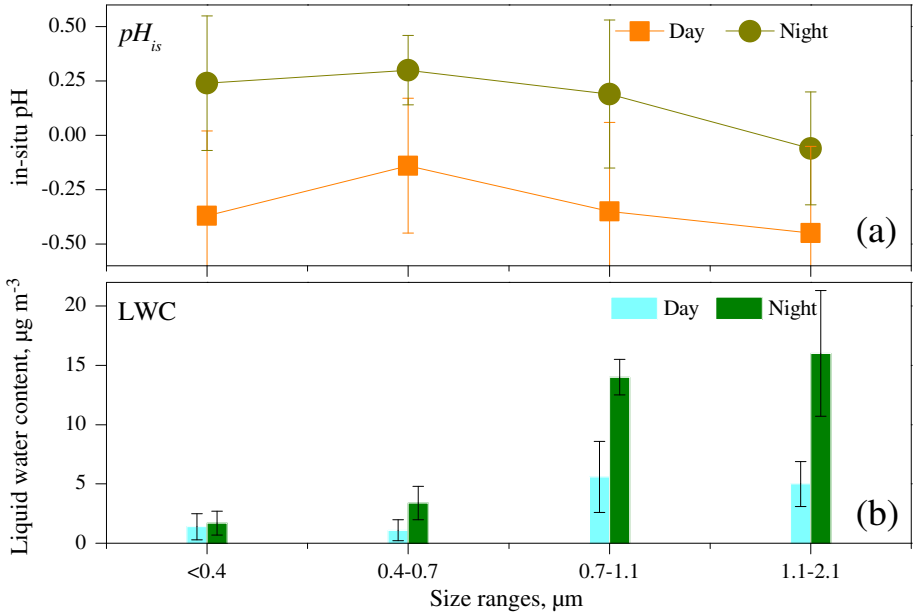

Fig. 3. Diurnal variations of (a) in-situ pH (pH_{is}) and (b) liquid water content (LWC) in the fine mode (<2.1 μm) samples from Chengdu.

2012). A robust linear correlation ($r^2 = 0.93$, $p < 0.01$) between K^+ and Cl^- was observed for the fine mode aerosols (Fig. 7a), suggesting that Cl^- was also emitted from biomass burning. Besides, the strong correlations of WSOC and WSON with K^+ (Fig. 7c and d) further indicate biomass burning emissions as important source of WSOC and WSON in the city in winter. Many researches have reported high concentrations of diacids in biomass burning plumes (Falkovich et al., 2005; Gao et al., 2003; Kundu et al., 2010; Miyazaki et al., 2009). In the present work C_2 and K^+ exhibited positive correlation in the fine mode aerosols (Fig. 7b), indicating an importance of precursors emitted from biomass burning and subsequent oxidation in the city. A robust correlation between K^+ (K^+/PM) and the ratio of $\omega C_2/C_2$ was only observed for the nighttime samples (Supplementary Fig. S4), which probably suggests that the production of C_2 from ωC_2 oxidation is enhanced due to biomass burning emissions.

4. Conclusions

Diurnal size-segregated aerosols in Chengdu, southwestern China, were collected from January 5th to 24th, 2011, and determined for dicarboxylic acids, ketocarboxylic acids, α-dicarbonyls, inorganic ions, WSOC and WSON. TSP-equivalent concentrations of total diacids were higher in nighttime (1831 ± 607 ng m^{-3}) than in daytime (1532 ± 196 ng m^{-3}), but the relative abundance of diacids to particle mass showed little diurnal difference (day: 0.36 ± 0.02%, night: 0.38 ± 0.1%). Both C_2 and C_4 showed a monomodal pattern with a dominant peak in the fine mode, while C_3

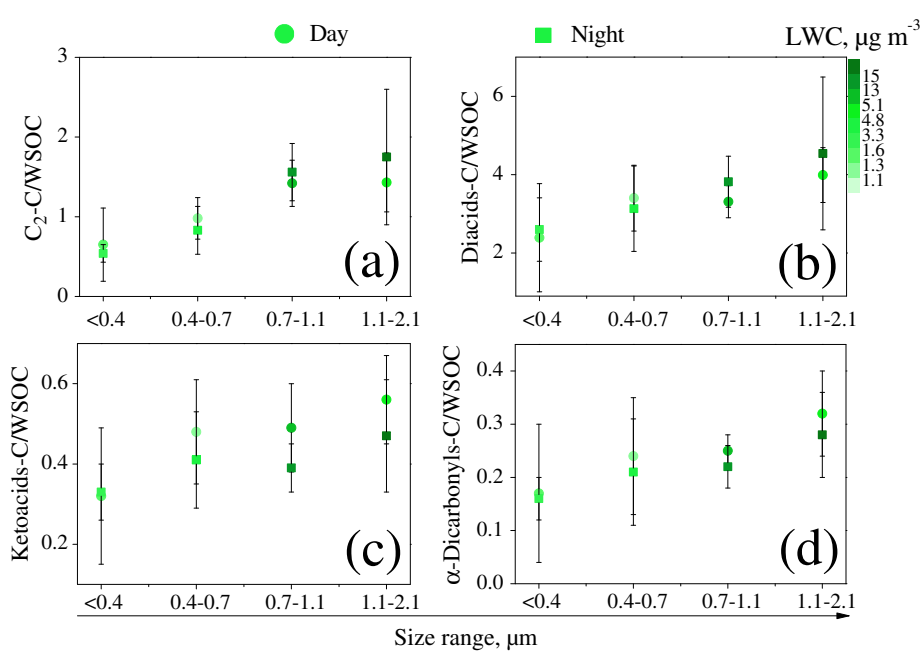

Fig. 4. Relative abundances of (a) oxalic acid (C_2), (b) diacids, (c) ketoacids and (d) α-dicarbonyls to water-soluble organic carbon (WSOC) on a carbon basis in the daytime and nighttime samples from Chengdu.

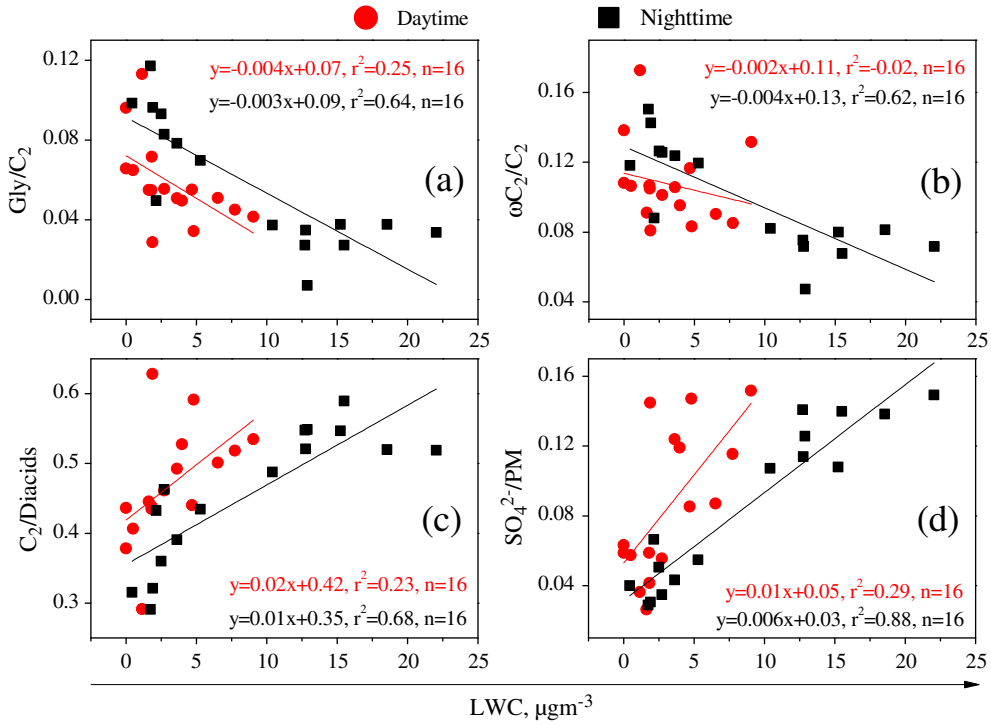

Fig. 5. Linear fit regressions for liquid water content (LWC) with (a) glyoxal/oxalic acid (Gly/C_2), (b) glyoxylic/oxalic acid ($\omega C_2/C_2$), (c) oxalic acid/diacids (C_2/diacids) and (d) SO_4^{2-} in the fine mode (<2.1 μm) samples from Chengdu.

exhibited a bimodal pattern with a large peak in the fine mode and a small peak in the coarse mode. Gly and mGly displayed a bimodal pattern, but Gly presented two equivalent peaks in the fine and coarse modes while mGly was dominant in the fine mode. LWC of the fine mode particles was three times higher in nighttime than in daytime, and the highest LWC was found in the size range 0.7–1.1 μm in daytime and in the larger size of 1.1–2.1 μm in nighttime. The calculated pH_{is} indicated that all the fine mode aerosols were acidic during the whole sampling period and more acidic in daytime than in nighttime. Pronounced linear correlations between Gly/C_2 and $\omega C_2/C_2$ with LWC were observed for the Chengdu fine samples, suggesting that the enhancement of LWC is favorable for C_2 production from Gly and ωC_2. Since enhanced LWC is favorable for the dissolution and partitioning of amines into the aqueous phase, an increase of WSON with an increase in LWC was found for the fine mode samples. Predominance of K^+ and Cl^- in the fine mode aerosols was associated with biomass burning emission, and the pronounced positive correlations of K^+ with WSOC, WSON and C_2, and their higher abundance in nighttime samples indicate that SOA in Chengdu is significantly affected by biomass burning emission.

Acknowledgments

This work was financially supported by the "Strategic Priority Research Program" of the Chinese Academy of Sciences (Grant Nos. XDA05100103, XDB05020401), China National Science Funds for Distinguished Young Scholars (Grant No. 41325014), and the State

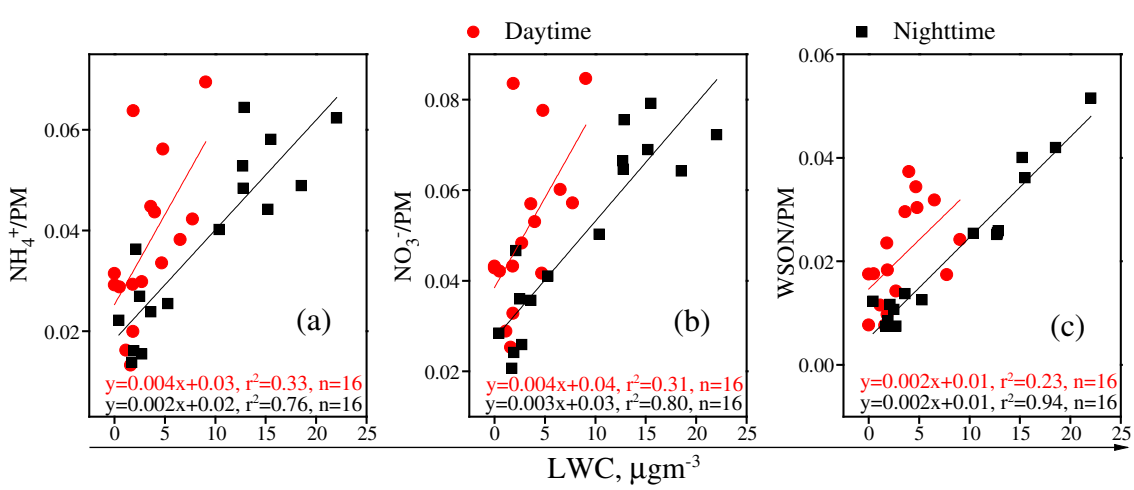

Fig. 6. Linear fit regressions for liquid water content (LWC) with mass fraction of (a) NH_4^+, (b) NO_3^- and (c) water-soluble organic nitrogen (WSON) in the fine mode (<2.1 μm) samples from Chengdu.

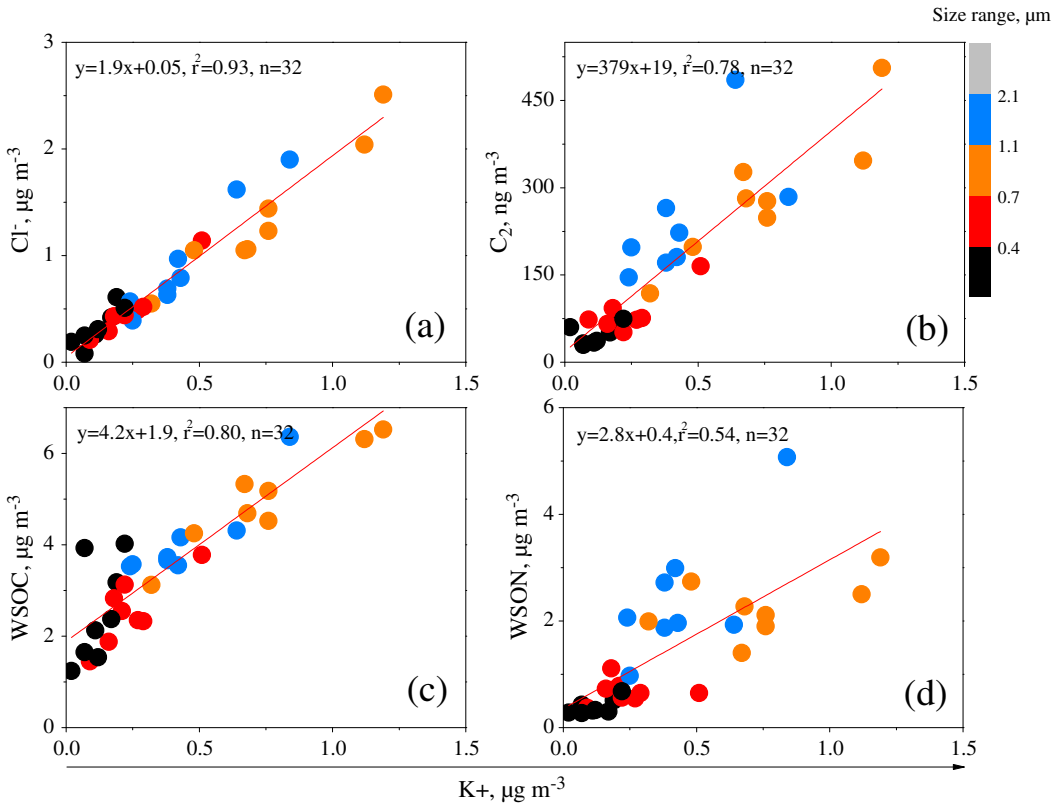

Fig. 7. Linear fit regressions for K^+ with (a) Cl^-, (b) oxalic acid (C_2), (c) water-soluble organic carbon (WSOC) and (d) water-soluble organic nitrogen (WSON) in the fine mode (<2.1 μm) samples from Chengdu.

Key Laboratory of Loess and Quaternary Geology open fund (SKLLQG1220).

Appendix A. Supplementary data

Supplementary data to this article can be found online at http://dx.doi.org/10.1016/j.atmosres.2015.04.010.

References

Agarwal, S., Aggarwal, S.G., Okuzawa, K., Kawamura, K., 2010. Size distributions of dicarboxylic acids, ketoacids, alpha-dicarbonyls, sugars, WSOC, OC, EC and inorganic ions in atmospheric particles over Northern Japan: implication for long-range transport of Siberian biomass burning and East Asian polluted aerosols. Atmos. Chem. Phys. 10, 5839–5858.

Andreae, M.O., 1983. Soot carbon and excess fine potassium — long-range transport of combustion-derived aerosols. Science 220, 1148–1151.

Cheng, C.L., Wang, G.H., Zhou, B.H., Meng, J.J., Li, J.J., Cao, J.J., Xiao, S., 2013. Comparison of dicarboxylic acids and related compounds in aerosol samples collected in Xi'an, China during haze and clean periods. Atmos. Environ. 81, 443–449.

Clegg, S.L., Brimblecombe, P., Wexler, A.S., 1998. Thermodynamic model of the system H^+–NH_4^+–SO_4^{2-}–NO_3–H_2O at tropospheric temperatures. J. Phys. Chem. A 102, 2137–2154.

Ervens, B., Gligorovski, S., Herrmann, H., 2003. Temperature-dependent rate constants for hydroxyl radical reactions with organic compounds in aqueous solutions. Phys. Chem. Chem. Phys. 5, 1811–1824.

Ervens, B., Turpin, B.J., Weber, R.J., 2011. Secondary organic aerosol formation in cloud droplets and aqueous particles (aqSOA): a review of laboratory, field and model studies. Atmos. Chem. Phys. 11, 11069–11102.

Ervens, B., Sorooshian, A., Lim, Y.B., Turpin, B.J., 2014. Key parameters controlling OH-initiated formation of secondary organic aerosol in the aqueous phase (aqSOA). J. Geophys. Res.-Atmos. 119, 3997–4016.

Falkovich, A.H., Graber, E.R., Schkolnik, G., Rudich, Y., Maenhaut, W., Artaxo, P., 2005. Low molecular weight organic acids in aerosol particles from Rondonia, Brazil, during the biomass-burning, transition and wet periods. Atmos. Chem. Phys. 5, 781–797.

Galloway, M.M., Chhabra, P.S., Chan, A.W.H., Surratt, J.D., Flagan, R.C., Seinfeld, J.H., Keutsch, F.N., 2009. Glyoxal uptake on ammonium sulphate seed aerosol: reaction products and reversibility of uptake under dark and irradiated conditions. Atmos. Chem. Phys. 9, 3331–3345.

Gao, S., Hegg, D.A., Hobbs, P.V., Kirchstetter, T.W., Magi, B.I., Sadilek, M., 2003. Water-soluble organic components in aerosols associated with savanna fires in southern Africa: identification, evolution, and distribution. J. Geophys. Res.-Atmos. 108.

Ge, X.L., Wexler, A.S., Clegg, S.L., 2011a. Atmospheric amines — part I. A review. Atmos. Environ. 45, 524–546.

Ge, X.L., Wexler, A.S., Clegg, S.L., 2011b. Atmospheric amines — part II. Thermodynamic properties and gas/particle partitioning. Atmos. Environ. 45, 561–577.

Ho, K.F., Cao, J.J., Lee, S.C., Kawamura, K., Zhang, R.J., Chow, J.C., Watson, J.G., 2007. Dicarboxylic acids, ketocarboxylic acids, and dicarbonyls in the urban atmosphere of China. J. Geophys. Res. Atmos. 112. http://dx.doi.org/10.1029/2006JD008011.

Huang, X.-F., Yu, J.Z., 2007. Is vehicle exhaust a significant primary source of oxalic acid in ambient aerosols? Geophys. Res. Lett. 34.

Jia, L., Xu, Y.F., 2014. Effects of relative humidity on ozone and secondary organic aerosol formation from the photooxidation of benzene and ethylbenzene. Aerosol Sci. Technol. 48, 1–12.

Jimenez, J.L., Canagaratna, M.R., Donahue, N.M., Prevot, A.S.H., Zhang, Q., Kroll, J.H., DeCarlo, P.F., Allan, J.D., Coe, H., Ng, N.L., Aiken, A.C., Docherty, K.S., Ulbrich, I.M., Grieshop, A.P., Robinson, A.L., Duplissy, J., Smith, J.D., Wilson, K.R., Lanz, V.A., Hueglin, C., Sun, Y.L., Tian, J., Laaksonen, A., Raatikainen, T., Rautiainen, J., Vaattovaara, P., Ehn, M., Kulmala, M., Tomlinson, J.M., Collins, D.R., Cubison, M.J., Dunlea, E.J., Huffman, J.A., Onasch, T.B., Alfarra, M.R., Williams, P.I., Bower, K., Kondo, Y., Schneider, J., Drewnick, F., Borrmann, S., Weimer, S., Demerjian, K., Salcedo, D., Cottrell, L., Griffin, R., Takami, A., Miyoshi, T., Hatakeyama, S., Shimono, A., Sun, J.Y., Zhang, Y.M., Dzepina, K., Kimmel, J.R., Sueper, D., Jayne, J.T., Herndon, S.C., Trimborn, A.M., Williams, L.R., Wood, E.C., Middlebrook, A.M., Kolb, C.E., Baltensperger, U., Worsnop, D.R., 2009. Evolution of organic aerosols in the atmosphere. Science 326, 1525–1529.

Kalberer, M., Paulsen, D., Sax, M., Steinbacher, M., Dommen, J., Prevot, A.S.H., Fisseha, R., Weingartner, E., Frankevich, V., Zenobi, R., Baltensperger, U., 2004. Identification of polymers as major components of atmospheric organic aerosols. Science 303, 1659–1662.

Kampf, C.J., Corrigan, A.L., Johnson, A.M., Song, W., Keronen, P., Konigstedt, R., Williams, J., Russell, L.M., Petaja, T., Fischer, H., Hoffmann, T., 2012. First measurements of reactive alpha-dicarbonyl concentrations on $PM_{2.5}$ aerosol over the Boreal forest in Finland during HUMPPA-COPEC 2010 — source apportionment and links to aerosol aging. Atmos. Chem. Phys. 12, 6145–6155.

Kawamura, K., Ikushima, K., 1993. Seasonal-changes in the distribution of dicarboxylic-acids in the urban atmosphere. Environ. Sci. Technol. 27, 2227–2235.

Kawamura, K., Ono, K., Tachibana, E., Charriere, B., Sempere, R., 2012. Distributions of low molecular weight dicarboxylic acids, ketoacids and alpha-dicarbonyls in the marine aerosols collected over the Arctic Ocean during late summer. Biogeosciences 9, 4725–4737.

Kawamura, K., Tachibana, E., Okuzawa, K., Aggarwal, S.G., Kanaya, Y., Wang, Z.F., 2013. High abundances of water-soluble dicarboxylic acids, ketocarboxylic acids and

alpha-dicarbonyls in the mountaintop aerosols over the North China Plain during wheat burning season. Atmos. Chem. Phys. 13, 8285–8302.
Kundu, S., Kawamura, K., Andreae, T.W., Hoffer, A., Andreae, M.O., 2010. Molecular distributions of dicarboxylic acids, ketocarboxylic acids and alpha-dicarbonyls in biomass burning aerosols: implications for photochemical production and degradation in smoke layers. Atmos. Chem. Phys. 10, 2209–2225.
Li, J., Wang, G., Zhou, B., Cheng, C., Cao, J., Shen, Z., An, Z., 2012. Airborne particulate organics at the summit (2060 m, a.s.l.) of Mt. Hua in central China during winter: implications for biofuel and coal combustion. Atmos. Res. 106, 108–119.
Lim, H.J., Turpin, B.J., 2002. Origins of primary and secondary organic aerosol in Atlanta: results of time-resolved measurements during the Atlanta supersite experiment. Environ. Sci. Technol. 36, 4489–4496.
Lim, H.J., Carlton, A.G., Turpin, B.J., 2005. Isoprene forms secondary organic aerosol through cloud processing: model simulations. Environ. Sci. Technol. 39, 4441–4446.
Lim, Y.B., Tan, Y., Perri, M.J., Seitzinger, S.P., Turpin, B.J., 2010. Aqueous chemistry and its role in secondary organic aerosol (SOA) formation. Atmos. Chem. Phys. 10, 10521–10539.
Lloyd, J.A., Heaton, K.J., Johnston, M.V., 2009. Reactive uptake of trimethylamine into ammonium nitrate particles. J. Phys. Chem. A 113, 4840–4843.
Malloy, Q.G.J., Qi, L., Warren, B., Cocker, D.R., Erupe, M.E., Silva, P.J., 2009. Secondary organic aerosol formation from primary aliphatic amines with NO_3 radical. Atmos. Chem. Phys. 9, 2051–2060.
Meng, J.J., Wang, G.H., Li, J.J., Cheng, C.L., Cao, J.J., 2013. Atmospheric oxalic acid and related secondary organic aerosols in Qinghai Lake, a continental background site in Tibet Plateau. Atmos. Environ. 79, 582–589.
Miyazaki, Y., Aggarwal, S.G., Singh, K., Gupta, P.K., Kawamura, K., 2009. Dicarboxylic acids and water-soluble organic carbon in aerosols in New Delhi, India, in winter: characteristics and formation processes. J. Geophys. Res.-Atmos. 114.
Myriokefalitakis, S., Tsigaridis, K., Mihalopoulos, N., Sciare, J., Nenes, A., Kawamura, K., Segers, A., Kanakidou, M., 2011. In-cloud oxalate formation in the global troposphere: a 3-D modeling study. Atmos. Chem. Phys. 11, 5761–5782.
Pavuluri, C.M., Kawamura, K., Swaminathan, T., 2010. Water-soluble organic carbon, dicarboxylic acids, ketoacids, and alpha-dicarbonyls in the tropical Indian aerosols. J. Geophys. Res.-Atmos. 115.
Prenni, A.J., DeMott, P.J., Kreidenweis, S.M., Sherman, D.E., Russell, L.M., Ming, Y., 2001. The effects of low molecular weight dicarboxylic acids on cloud formation. J. Phys. Chem. A 105, 11240–11248.
Salo, K., Westerlund, J., Andersson, P.U., Nielsen, C., D'Anna, B., Hallquist, M., 2011. Thermal characterization of aminium nitrate nanoparticles. J. Phys. Chem. A 115, 11671–11677.
Sellegri, K., Hanke, M., Umann, B., Arnold, F., Kulmala, M., 2005. Measurements of organic gases during aerosol formation events in the boreal forest atmosphere during QUEST. Atmos. Chem. Phys. 5, 373–384.
Shiraiwa, M., Yee, L.D., Schilling, K.A., Loza, C.L., Craven, J.S., Zuend, A., Ziemann, P.J., Seinfeld, J.H., 2013. Size distribution dynamics reveal particle-phase chemistry in organic aerosol formation. Proc. Natl. Acad. Sci. U. S. A. 110, 11746–11750.
Silva, P.J., Erupe, M.E., Price, D., Elias, J., Malloy, Q.G.J., Li, Q., Warren, B., Cocker, D.R., 2008. Trimethylamine as precursor to secondary organic aerosol formation via nitrate radical reaction in the atmosphere. Environ. Sci. Technol. 42, 4689–4696.
Stone, E.A., Hedman, C.J., Zhou, J.B., Mieritz, M., Schauer, J.J., 2010. Insights into the nature of secondary organic aerosol in Mexico City during the MILAGRO experiment 2006. Atmos. Environ. 44, 312–319.
Tan, Y., Carlton, A.G., Seitzinger, S.P., Turpin, B.J., 2010. SOA from methylglyoxal in clouds and wet aerosols: measurement and prediction of key products. Atmos. Environ. 44, 5218–5226.
Tao, J., Zhang, L., Engling, G., Zhang, R., Yang, Y., Cao, J., Zhu, C., Wang, Q., Luo, L., 2013. Chemical composition of $PM_{2.5}$ in an urban environment in Chengdu, China: importance of springtime dust storms and biomass burning. Atmos. Res. 122, 270–283.
van Donkelaar, A., Martin, R.V., Brauer, M., Kahn, R., Levy, R., Verduzco, C., Villeneuve, P.J., 2010. Global estimates of ambient fine particulate matter concentrations from satellite-based aerosol optical depth: development and application. Environ. Health Perspect. 118, 847–855.
van Pinxteren, D., Neususs, C., Herrmann, H., 2014. On the abundance and source contributions of dicarboxylic acids in size-resolved aerosol particles at continental sites in central Europe. Atmos. Chem. Phys. 14, 3913–3928.
Vrekoussis, M., Wittrock, F., Richter, A., Burrows, J.P., 2009. Temporal and spatial variability of glyoxal as observed from space. Atmos. Chem. Phys. 9, 4485–4504.
Wang, G.H., Kawamura, K., Lee, S., Ho, K.F., Cao, J.J., 2006. Molecular, seasonal, and spatial distributions of organic aerosols from fourteen Chinese cities. Environ. Sci. Technol. 40, 4619–4625.
Wang, G., Xie, M., Hu, S., Gao, S., Tachibana, E., Kawamura, K., 2010. Dicarboxylic acids, metals and isotopic compositions of C and N in atmospheric aerosols from inland China: implications for dust and coal burning emission and secondary aerosol formation. Atmos. Chem. Phys. 10, 6087–6096.
Wang, G., Kawamura, K., Xie, M., Hu, S., Li, J., Zhou, B., Cao, J., An, Z., 2011. Selected water-soluble organic compounds found in size-resolved aerosols collected from urban, mountain and marine atmospheres over East Asia. Tellus Ser. B Chem. Phys. Meteorol. 63, 371–381.
Wang, G., Kawamura, K., Cheng, C., Li, J., Cao, J., Zhang, R., Zhang, T., Liu, S., Zhao, Z., 2012a. Molecular distribution and stable carbon isotopic composition of dicarboxylic acids, ketocarboxylic acids, and alpha-dicarbonyls in size-resolved atmospheric particles from Xi'an City, China. Environ. Sci. Technol. 46, 4783–4791.
Wang, G., Li, J., Cheng, C., Zhou, B., Xie, M., Hu, S., Meng, J., Sun, T., Ren, Y., Cao, J., 2012b. Observation of atmospheric aerosols at Mt. Hua and Mt. Tai in central and east China during spring 2009 — part 2: impact of dust storm on organic aerosol composition and size distribution. Atmos. Chem. Phys. 12, 4065–4080.
Wang, G.H., Zhou, B.H., Cheng, C.L., Cao, J.J., Li, J.J., Meng, J.J., Tao, J., Zhang, R.J., Fu, P.Q., 2013a. Impact of Gobi desert dust on aerosol chemistry of Xi'an, inland China during spring 2009: differences in composition and size distribution between the urban ground surface and the mountain atmosphere. Atmos. Chem. Phys. 13, 819–835.
Wang, Q., Cao, J., Shen, Z., Tao, J., Xiao, S., Luo, L., He, Q., Tang, X., 2013b. Chemical characteristics of $PM_{2.5}$ during dust storms and air pollution events in Chengdu, China. Particuology 11, 70–77.
Wang, Y., Zhang, Q.Q., He, K., Zhang, Q., Chai, L., 2013c. Sulfate–nitrate–ammonium aerosols over China: response to 2000–2015 emission changes of sulfur dioxide, nitrogen oxides, and ammonia. Atmos. Chem. Phys. 13, 2635–2652.
Wexler, A.S., Clegg, S.L., 2002. Atmospheric aerosol models for systems including the ions H^+, NH_4^+, Na^+, SO_4^{2-}, NO_3^-, Cl^-, Br^-, and H_2O. J. Geophys. Res.-Atmos. 107.
Xue, J., Lau, A.K.H., Yu, J.Z., 2011. A study of acidity on $PM_{2.5}$ in Hong Kong using online ionic chemical composition measurements. Atmos. Environ. 45, 7081–7088.
Yang, L.M., Ray, M.B., Yu, L.E., 2008. Photooxidation of dicarboxylic acids — part II: kinetics, intermediates and field observations. Atmos. Environ. 42, 868–880.
Yang, Y., Chan, C.-y., Tao, J., Lin, M., Engling, G., Zhang, Z., Zhang, T., Su, L., 2012. Observation of elevated fungal tracers due to biomass burning in the Sichuan Basin at Chengdu City, China. Sci. Total Environ. 431, 68–77.
Yasmeen, F., Sauret, N., Gal, J.F., Maria, P.C., Massi, L., Maenhaut, W., Claeys, M., 2010. Characterization of oligomers from methylglyoxal under dark conditions: a pathway to produce secondary organic aerosol through cloud processing during nighttime. Atmos. Chem. Phys. 10, 3803–3812.
Zhang, X.Y., Wang, Y.Q., Niu, T., Zhang, X.C., Gong, S.L., Zhang, Y.M., Sun, J.Y., 2012. Atmospheric aerosol compositions in China: spatial/temporal variability, chemical signature, regional haze distribution and comparisons with global aerosols. Atmos. Chem. Phys. 12, 779–799.